Graded-Index-Fiber-Inspired 3-D Printed Surface Focusing Porous Dielectric Structure With GaAs MMIC Rectenna Toward Millimeter-Wave Wireless Power Transfer Application

Wenyi Shao, *Member, IEEE*, Bo Yang, Naoki Sakai, *Member, IEEE*, Tsukasa Hirai, Kenji Itoh, *Fellow, IEEE*, Qiang Chen, *Senior Member, IEEE*, and Naoki Shinohara, *Senior Member, IEEE*

***Abstract*—Borrowing the idea of the graded-index (GRIN) fiber, we propose an all-dielectric porous structure with a unique surface focusing feature to improve the performance of the rectenna for millimeter-wave (mm-Wave) wireless power transfer (WPT) applications in this letter. The on- and off-axis focusing properties of the proposed structure are analyzed by the full-wave electromagnetic simulation. Moreover, benefitting from the low-cost 3-D printing technique, the designed GRIN structure prototype with different pore densities of the polylactic acid material is fabricated. The near-field phase transform experiment at 28 GHz was carried out to verify the excellent focusing performance of the fabricated structure prototype. Besides, the characteristics of multifocal spots on the surface of the proposed structure are further confirmed by the mm-Wave WPT experiments with a GaAs monolithic microwave integrated circuit rectenna using a 0.5 μm enhancement-mode pseudomorphic-HEMT gated anode diode, which reveals the great potential of the proposed structure for improving the applicability of the rectenna array in practical mm-Wave WPT applications by reducing its sensitivity to an incident angle of the transmitted beam.**

***Index Terms*—Additive manufacturing, double voltage rectifier, millimeter-wave, wireless power transfer.**

I. Introduction

With the explosive growth of Internet-of-Things (IoT) devices supported by the millimeter-wave (mm-Wave) technology beyond 5G and 6G networks, there is a growing need for wireless power transfer (WPT) techniques to provide a convenient solution to power and recharge these devices. Compared to the traditional WPT systems [1], [2], [3], [4] operating at 2.45 and 5.8 GHz, mm-Wave WPT systems offer some advantages such as ultrahigh-speed communications while charging [5], [6] and a higher end-to-end wireless energy transfer efficiency at mm-Wave bands.

But, as one of the most important components in the mmWave WPT system, the performance of the rectenna is easily affected by the variation of the load resistance and the input power level, which still limits the overall performance of the mm-Wave WPT system [7] at present. Various impedance-matching network topologies [8], [9], [10] can be developed to maintain stable efficiency within a certain load range. However, due to the divergence characteristic of the transmitted radiation beam in the free space, higher spillover loss occurs [11] for long-range transmission. It means the RF power of the transmitted radiation beam captured by the rectenna is very low and varies with locations in practical long-range WPT applications. Besides, the misalignment between the transmitting antenna and receiving rectenna also further reduces the performance of the rectenna. Several focusing components, such as homogenous lens [12] and metasurface [13], [14], have been proposed to solve these problems by concentrating divergent transmitted beams to enhance the incident RF power at the rectenna. Although metasurface has the advantages of being lightweight and low profile compared to dielectric lenses, the focusing principles behind these two methods are the same and based on the concepts of optical lenses. By manipulating the wavefront on the antenna aperture, both of these can achieve the superposition of the field in phase at the focal point. It also means additional space is required to place the rectenna in these two methods, which can result in larger device sizes and less system integration. As a special type of optical lens, the graded-index (GRIN) lens represented by the Luneburg lens has a nonuniform and special refractive index profile, resulting in unique focusing properties. The Luneburg lens can focus the transmitted beam from all directions equally well on its surface. However, the spherical shape feature of the Luneburg lens [15] brings difficulties in integrating the planar array rectenna on its surface. An additional and complex transformation optics (TO) method is required to flatten its spherical shape.

Inspired by the autofocusing GRIN fiber as shown in Fig. 1, a surface-focusing dielectric structure at 28 GHz is proposed for solving these problems in this letter. The period of the rays inside the fiber is defined as pitch (P). Surface-focusing features can be obtained by selecting $P = 0.25$ according to

Manuscript received 12 July 2023; revised 3 September 2023; accepted 5 September 2023. Date of publication 7 September 2023; date of current version 1 December 2023. This work was supported in part by the Microwave Energy Transmission Laboratory (METLAB), Research Institute for Sustainable Humanosphere, Kyoto University, and in part by the National Institute of Information and Communications Technology (NICT), Japan, under Grant 02401. *(Corresponding author: Bo Yang.)*

Wenyi Shao, Bo Yang, and Naoki Shinohara are with the Research Institute for Sustainable Humanosphere, Kyoto University, Uji 611-0011, Japan (e-mail: shao.wenyi.6r@kyoto-u.ac.jp; yang.bo.82x@kyoto-u.jp; shino@rish.kyoto-u.ac.jp).

Naoki Sakai, Tsukasa Hirai, and Kenji Itoh are with the Kanazawa Institute of Technology, Nonoichi 921-8510, Japan (e-mail: naoki.sakai@neptune.kanazawa-it.ac.jp; b6200754@st.kanazawa-it.ac.jp; itoh.kenji@ieee.org).

Qiang Chen is with the Department of Communications Engineering, Tohoku University, Sendai 980-8579, Japan (e-mail: qiang.chen.a5@tohoku.ac.jp).

Digital Object Identifier 10.1109/LAWP.2023.3312691

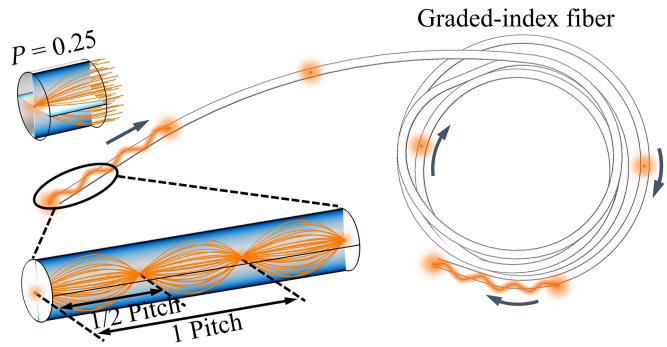

Fig. 1. Characteristic of autofocusing GRIN optical fiber. $P = 0.25$: surface focusing.

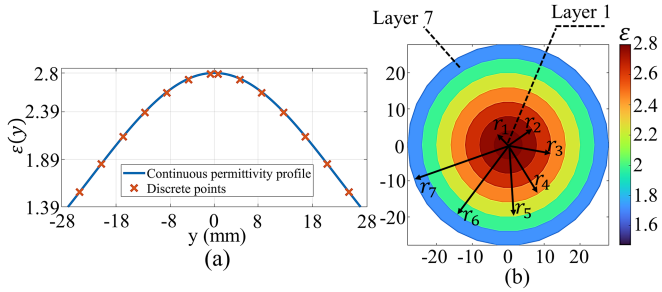

Fig. 2. (a) Discretization of a 1-D continuous permittivity profile of the proposed surface focusing structure. (b) 2-D discrete permittivity distribution of the proposed structure: $r_1 = 4$ mm, $r_2 = 8$ mm, $r_2 = 12$ mm, $r_4 = 16$ mm, $r_5 = 20$ mm, $r_6 = 24$ mm, and $r_7 = 28$ mm.

the principle of light reversibility. Unlike the Luneburg lens, the proposed structure has a flat shape with a unique surface focusing feature, which does not require complex approaches, such as TO [16], [17], to flatten its original shape. Moreover, compared with a homogenous lens and a metasurface, the planar rectenna array can be also easily integrated on the surface of the proposed structure to shrink the space of the entire received system, and each rectenna in the array would receive highly concentrated RF power from a specific direction. Besides, unlike the conventional rectifier circuit design based on GaAs Schottky barrier diodes (SBDs), the 0.5 μm GaAs enhancement-mode pseudomorphic-HEMT (E-pHEMT) gated anode diode (GAD) is utilized for achieving high-power rectification. In order to simplify the rectifier circuit design, the impedance-matching circuit is removed by directly conjugate matching the impedance of the patch antenna with the rectifier.

II. Design of Surface Focusing Porous Structure

A. Porous Structure Realization Using 3-D Printing

The transverse permittivity profile (hyperbolic cosine) of the surface focusing structure as shown in Fig. 2(a) is defined by the following equation [18]:

$$\varepsilon(y) = \frac{\varepsilon_0}{\cosh^2(\alpha y)} \tag{1}$$

where ε_0 is the central permittivity. $\alpha = 2\pi P/w$ is the gradient parameter. $w$is the width of the designed focusing structure. P is the pitch.

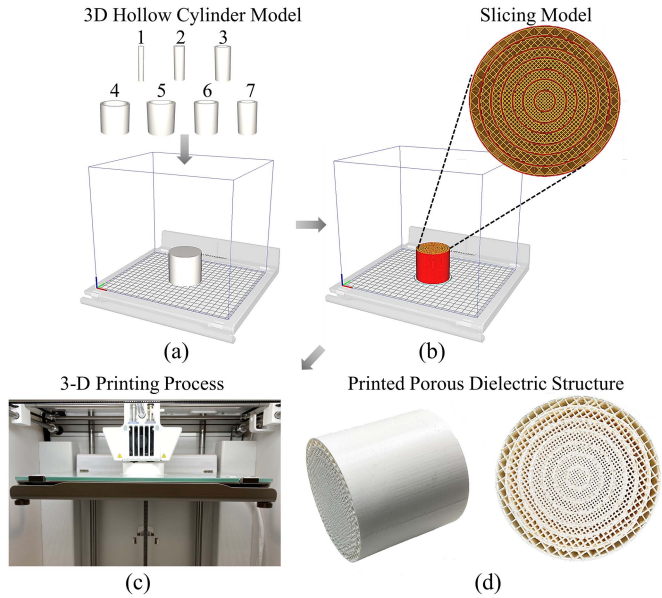

Fig. 3. Design procedure of the proposed surface focusing structure at 28 GHz. (a) Seven hollow cylinders model preparation. (b) 3-D slicing. (c) 3-D printing process. (d) Fabricated prototype.

Here, the desired permittivity profile of the proposed surface-focusing structure can be easily achieved by using porous layers with different infill ratios. The pitch (P), aperture diameter (D), and width (w) of the proposed structure are 0.25, 56 mm, and 52 mm, respectively. The 1-D continuous permittivity profile of the proposed structure needs to be first discretized into seven discrete points with the corresponding permittivity of 1.55, 1.84, 2.13, 2.38, 2.59, 2.73, and 2.7, as shown in Fig. 2(a). The 2-D discrete permittivity distribution with a uniform spacing of 4 mm is illustrated in Fig. 2(b). The different colors represent the corresponding discrete values of permittivity. Then, by controlling the infill ratios (v) of 3-D printing dielectric materials, the values of equivalent permittivity (ε_{eff}) for different discrete layers can be obtained by [18]

$$\varepsilon_{\text{eff}} = 1 + v(\varepsilon_m - 1) \tag{2}$$

where ε_m is the relative permittivity of the polylactic acid (PLA) plastic material ($\varepsilon_m = \sim 2.8$, $\tan\delta = \sim 0.019$).

Fig. 3 illustrates the specific design procedure of the proposed surface focusing structure at 28 GHz. First, the open-source Ultimaker Cura 3-D slicing software is utilized to combine seven hollow cylinders with different radii into one model and form a 3-D slicing model with different ratios (from layer No. 1 to 7: 99.3%, 96%, 88.3%, 76.8%, 62.6%, 46.7%, and 30.3%) for each hollow cylinder, as shown in Fig. 3(a) and (b). The setting of layer height is 0.06 mm, and the print time is about 10 h. Fig. 3(c) and (d) shows the fabricated prototype of the proposed structure operating at 28 GHz with an aperture diameter of 56 mm and a length of 52 mm.

B. Surface Focusing Analysis

Because the geometrical optics is the asymptotic solution of Maxwell's equations, the focusing performance of the proposed structure is verified by using full-wave simulation in CST Microwave Studio instead of the ray-tracing method [20]

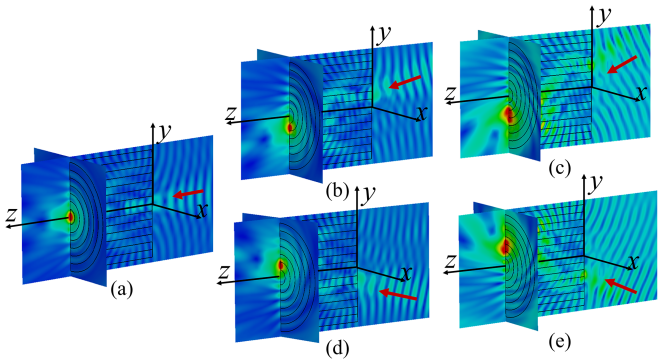

Fig. 4. Surface focusing analysis based on full-wave simulation for different incidence angles of (a) 0°. (b) 15°. (c) 30°. (d) −15°. (e) −30°.

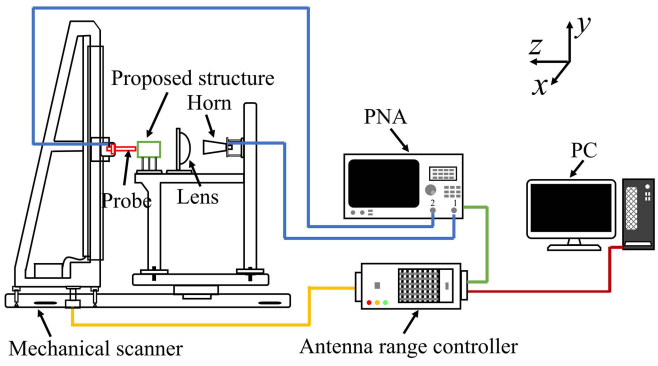

Fig. 5. Schematic view of measurement setups for a near-field phase transform experiment at 28 GHz.

in our case. The simulation model for the proposed focusing structure at 28 GHz consists of seven concentric dielectric cylinders with permittivity of 1.55, 1.84, 2.13, 2.38, 2.59, 2.73, and 2.79, respectively. The plane wave excitation with different incident angles is set. Considering that the proposed structure is symmetry around the center axis, Fig. 4(a)–(e) only gives five examples of the simulated 2-D electric field distribution inside the proposed structure at 28 GHz with different incident angles of 0°, ±15°, and ±30° for the sake of brevity. After propagating through the proposed structure, the plane waves can be well concentrated into a focusing spot on the surface of the proposed structure ($z = 52$ mm). Besides, other phenomena such as interface reflection at plane of $z = 0$ mm can also be well observed. Overall, the simulated results indicate that proposed structure design at 28 GHz can be a good phase transformer to convert plane waves with different incident angles into the different focusing spots on the surface of the proposed structure.

C. Near-Field Phase Transform Experimental Verification

Fig. 5 shows measurement setups of the near-field phase transform experiment for validating the surface-focusing characteristic of the proposed structure. A plano-convex hyperbolic dielectric lens [21] with a WR-34 standard horn antenna feeding source is utilized to generate an approximate plane wave in the near field. The waveguide probe is fixed on the mechanical scanner and can be moved along horizontal and vertical directions step by step to obtain the E-field at the rear surface of the proposed structure. In our case, to shorten the test time,

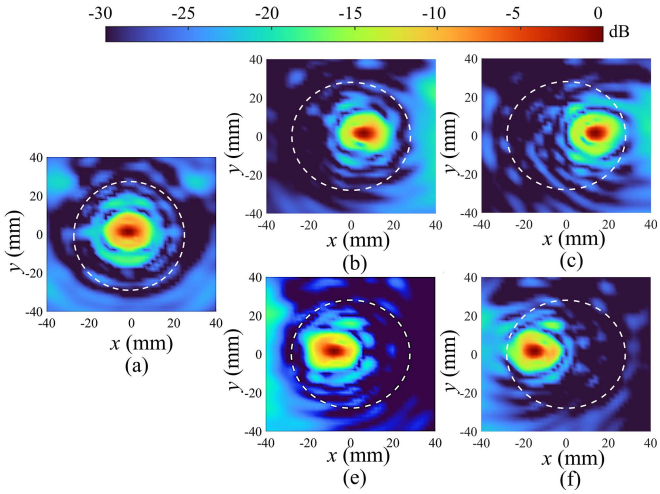

Fig. 6. Measured normalized 2-D electric field distribution at the rear surface of the proposed focusing structure at 28GHz with different incident angles of a generated approximate plane wave. Note that the white dotted circle represents the actual physical aperture (56 mm) of the proposed focusing structure.

the size of the entire scanning area is 80 mm × 80 mm, and the distance of each movement for the 2-D linear guide rail is set to 2 mm. Besides, the plano-convex hyperbolic lens and horn antenna are rotated simultaneously around the y-axis to generate the plane wave with different incident angles. When the lens and horn antenna simultaneously rotate counterclockwise, the focusing spot starts from the initial position $x = 0$ and moves along the positive half of the x-axis, as shown in Fig. 6(a)–(c). Likewise, the clockwise rotation of the lens and horn antenna produces a focusing spot that moves along the negative half of the x-axis, as shown in Fig. 6(e) and (f). This indirectly indicates the proposed structure can converge electromagnetic waves from a long distance with different incident directions in free space.

III. Wireless Power Transfer Experiment

To further demonstrate that the surface-focusing feature of the proposed structure can improve the performance of the rectenna, we conducted a wireless power transfer experiment with a GaAs monolithic microwave integrated circuit (MMIC) rectenna at 28 GHz. Fig. 7 illustrates measurement setups of the wireless power transfer experiment. The RF signal generator (Keysight N5173B) can generate CW signals up to 40 GHz. The generated RF signals are increased by an RF power amplifier (AMP6034-40, Exodus Advanced Communications) to provide RF input signals with different powers. Here, the WR-34 standard horn antenna and lens are combined to form a transmitting antenna. The fabricated GaAs MMIC rectenna prototype [22] at 28 GHz is deployed on the dielectric substrate with a relative permittivity of 3.6, a loss tangent of 0.0015, and a thickness of 0.625 mm. It consists of two main parts: 1) double voltage rectifier and 2) inductive patch antenna with high impedance. Both parts are integrated on the GaAs chip with a size of 1.8 mm × 1.8 mm × 0.1 mm. In order to achieve high-power and high-efficiency rectification, unlike the rectifier circuit design based on conventional GaAs SBDs in previous studies, the 0.5 μm GaAs E-pHEMT GAD [22], [23] is applied in the rectifier circuit. Besides, there are no impedance-matching circuits between the radiated patch antenna and the rectifier

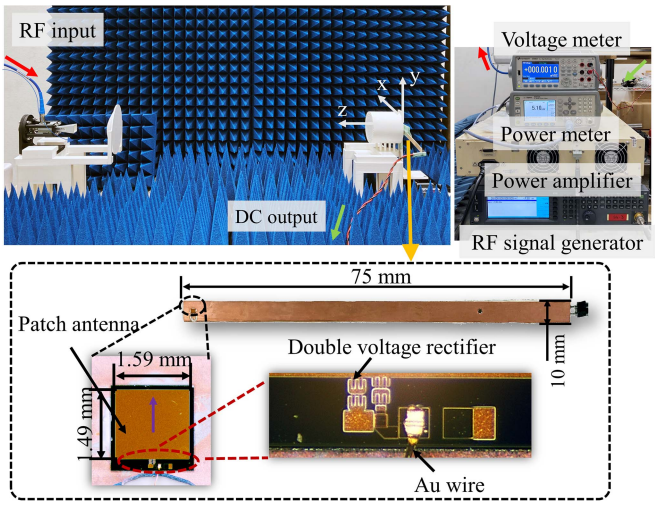

Fig. 7. Photograph of the measurement setups of the wireless power transfer experiment with a GaAs MMIC rectenna at 28 GHz.

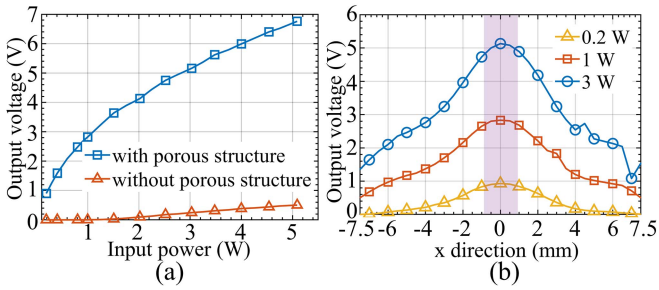

Fig. 8. (a) Measured dc output voltage for different input powers with and without the proposed structure. (b) Measured dc output voltage for different positions on the x-axis with the proposed structure under different input powers.

circuit to simplify the design. The patch antenna impedance is directly conjugate-matched with the rectifier. The calculated maximum rectification efficiency for the rectifier circuit is 55% with an input power of 27.9 dBm for a 3.0 kΩ load. Note that the purple arrow represents the polarization direction of the rectenna. The proposed GaAs MMIC rectenna is fixed on a high-precision linear motor (ALZ-4011-GOM, CHUO Precision Industrial) and can be moved back and forth along the x-axis from $x = -7.5$ mm to $x = 7.5$ mm. The dc output voltage from the rectifier circuit is measured by a digital multimeter.

Fig. 8(a) shows the measured dc output voltage under different input powers for the horn antenna from 22.8 dBm to 37.1 dBm with and without the proposed structure. In both cases, the dc output voltage increases with the input power. However, owing to the focusing feature of the proposed structure, the received power density of the rectenna is increased, which significantly further increases the dc output voltage. For example, when the input power and the resistive load is 37.1 dBm and 3.0 kΩ, the dc output voltage is 6.76 V with the proposed structure, which is about 13 times that of the case (502 mV) without the proposed structure. Besides, to verify the focusing performance of the proposed structure, the rectenna is moved along the x-axis from $x = -7.5$ mm to $x = 7.5$ mm by controlling the linear motor. The measured dc output voltage for different positions on the x-axis with different input powers is given in Fig. 8(b). Obviously, the dc output voltage has only one peak along the

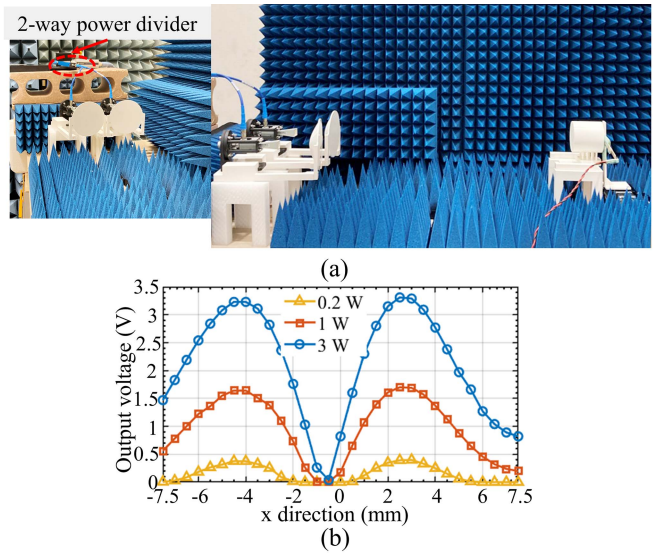

Fig. 9. (a) Photograph of measurement setups of the WPT experiment with dual transmitters at 28 GHz. (b) Measured dc output voltage for different positions on the x-axis under different input powers.

x-axis. It also demonstrates that the focusing performance is well obtained owing to the good phase transformation function of the proposed structure. Besides, as mentioned in Section II, the position of the focal spot changes with the incident angles of the transmitted beam. To verify the characteristics of multifocal spots of the proposed structure, two same transmitters with different orientations are used in the WPT experiment, as shown in Fig. 9(a). The two-way power divider is utilized to connect these two transmitters. Two transmitted beams generated by two transmitters have different incident angles. After propagating through the proposed structure, these two beams are focused, and formed into two separate focal spots on the surface of the proposed structure, respectively. Fig. 9(b) shows the measured dc output voltage for different positions on the x-axis with different RF input powers. As expected, there are two separate peaks in the dc output voltage curves as the rectenna moves along the x-axis. Two focusing spots generated by the proposed structure greatly increase the input power density level for the rectenna, which leads to the formation of two peaks of the output dc voltage. This proves the possibility for a rectenna array to reduce sensitivity to an incident angle of the radiated beam by using the proposed structure.

IV. Conclusion

An all-dielectric porous structure with a unique surface focusing at 28 GHz was proposed and fabricated to improve the performance of the rectenna for mm-Wave WPT applications in this letter. The near-field phase transform experiment was carried out to demonstrate the excellent phase transformation function of the proposed structure with different incident angles of the generated plane wave at 28 GHz. Besides, in the mm-Wave WPT experiment, a GaAs MMIC rectenna using (E-pHEMT) GAD at 28 GHz is utilized. The measurement results indicate the transmitted RF beam can be well focused on the surface of the rectenna and the dc output voltage can be significantly increased. Most importantly, the characteristics of multifocal spots of the proposed structure can be achieved.

REFERENCES

[1] N. Shinohara, "Power without wires," *IEEE Microw. Mag.*, vol. 12, no. 7, pp. S64–S73, Dec. 2011.

[2] X. Duan, L. Zhou, Y. Zhou, Y. Tang, and X. Chen, "Short-distance wireless power transfer based on microwave radiation via an electromagnetic rectifying surface," *IEEE Antennas Wireless Propag. Lett.*, vol. 19, no. 12, pp. 2344–2348, Dec. 2020.

[3] Y. Tanaka et al., "Simulation and implementation of distributed microwave wireless power transfer system," *IEEE Trans. Microw. Theory Techn.*, vol. 71, no. 1, pp. 102–111, Jan. 2023.

[4] B. Yang, T. Mitani, and N. Shinohara, "Auto-tracking wireless power transfer system with focused-beam phased array," *IEEE Trans. Microw. Theory Techn.*, vol. 71, no. 5, pp. 2299–2306, May 2023.

[5] A. A. Aziz et al., "Battery-less location tracking for Internet of Things: Simultaneous wireless power transfer and positioning," *IEEE Internet Things J.*, vol. 6, no. 5, pp. 9147–9164, Oct. 2019.

[6] C. T. Rodenbeck et al., "Microwave and millimeter wave power beaming," *IEEE J. Microw.*, vol. 1, no. 1, pp. 229–259, Jan. 2021.

[7] S. Ladan, A. B. Guntupalli, and K. Wu, "A high-efficiency 24 GHz rectenna development towards millimeter-wave energy harvesting and wireless power transmission," *IEEE Trans. Circuits Syst. I, Reg. Papers*, vol. 61, no. 12, pp. 3358–3366, Dec. 2014.

[8] J. Chen, H. Xiao, H. Xiong, D. Xiao, W. Song, and H. Zhang, "An impedance matcher for microwave rectifier to broaden load range," *IEEE Microw. Wireless Compon. Lett.*, vol. 32, no. 10, pp. 1215–1218, Oct. 2022.

[9] X. Y. Zhang, Z.-X. Du, and Q. Xue, "High-efficiency broadband rectifier with wide ranges of input power and output load based on branch-line coupler," *IEEE Trans. Circuits Syst. I, Reg. Papers*, vol. 64, no. 3, pp. 731–739, Mar. 2017.

[10] Y. Zheng, S. H. Wang, K. W. Leung, W. S. Chan, and M. H. Xia, "A high-efficiency rectifier with ultra-wide input power range based on cooperative structure," *IEEE Trans. Microw. Theory Techn.*, vol. 67, no. 11, pp. 4524–4533, Nov. 2019.

[11] R. A. M. Pereira and N. B. Carvalho, "Quasioptics for increasing the beam efficiency of wireless power transfer systems," *Sci. Rep.*, vol. 12, no. 1, Dec. 2022, Art. no. 20894.

[12] A.-H. Hobballah, R. Négrier, and M. Lalande, "A dielectric lens rectenna for wireless power transmission," in *Proc. 51st Eur. Microw. Conf.*, 2022, pp. 672–675.

[13] X. Wu et al., "Accurate and efficient method for analyzing the transfer efficiency of metasurface-based wireless power transfer system," *IEEE Trans. Antennas Propag.*, vol. 71, no. 1, pp. 783–795, Jan. 2023.

[14] X. Wang, M. S. Tong, and G.-M. Yang, "Multifocus multinull near-field transmitting focused metasurface," *IEEE Trans. Antennas Propag.*, vol. 71, no. 4, pp. 3172–3182, Apr. 2023.

[15] S. S. Vinnakota, R. Kumari, H. Meena, and B. Majumder, "Rectifier integrated multibeam Luneburg lens employing artificial dielectric as a wireless power transfer medium at mm wave band," *IEEE Photon. J.*, vol. 13, no. 3, Jun. 2021, Art. no. 5500314.

[16] Y. H. Lou, Y. X. Zhu, G. F. Fan, W. Lei, W. Z. Lu, and X. C. Wang, "Design of Ku-band flat Luneburg lens using ceramic 3-D printing," *IEEE Antennas Wireless Propag. Lett.*, vol. 20, no. 2, pp. 234–238, Feb. 2021.

[17] R. Xu and Z. N. Chen, "A transformation-optics-based flat metamaterial Luneburg lens antenna with zero focal length," *IEEE Trans. Antennas Propag.*, vol. 70, no. 5, pp. 3287–3296, May 2022.

[18] A. L. Mikaelian, "Self-focusing medium with variable index of refraction," in *Progress in Optics XVII*, E. Wolf, Ed. Amsterdam, The Netherlands: North Holland, 1980.

[19] J. Pourahmadazar and T. A. Denidni, "Towards millimeter-wavelength: Transmission-mode Fresnel-zone plate lens antennas using plastic material porosity control in homogeneous medium," *Sci. Rep.*, vol. 8, no. 1, pp. 1–14, Jan. 2018.

[20] C. Gomez-Reino, M. V. Perez, and C. Bao, *Gradient-Index Optics: Fundamentals and Applications*. New York, NY, USA: Springer, 2002, pp. 128–131.

[21] J. J. Lee, "Lens antennas," in *Antenna Handbook*. New York, NY, USA: Van Nostrand Reinhold, 1988.

[22] T. Hirai et al., "28 GHz band wireless power transfer experiments with a GaAs rectenna MMIC with an inductive high impedance patch antenna," in *Proc. IEEE Asia-Pacific Microw. Conf.*, 2022, pp. 731–733.

[23] N. Kakutani, F. Komatsu, N. Sakai, and K. Itoh, "30 GHz band double voltage rectifier MMIC with the 0.1 μm E-pHEMT gated anode diode," in *Proc. IEEE Asia-Pacific Microw. Conf.*, 2022, pp. 449–451.